scientific reports

Check for updates

OPEN

Projecting the effect of climate change on multiple Geomorphological hazard using machine learning data driven approaches

Narges Kariminejad[1], Atiyeh Amindin[2], Adel Sepehr[3] & Hamid Reza Pourghasemi[2]✉

Land subsidence (LS) and collapsed pipes (CP) pose environmental and socio-economic threats in arid and semi-arid regions. This study assesses the effect of climate change to address these problems in Khorasan-Razavi province, Iran. Thus, we mapped soil landforms susceptible to LS and CP based on climatic, geolocic, topoghraphic, hydrologic and edaphic variables using an ensemble forecasting approach. Additionally, we predicted the future susceptibility of CP and LS based on two future emission scenario pathways (SSP 5-8.5 and SSP 1-2.6), in 2030, 2050, 2070, and 2090. The assessment showed that the area under the ROC curve (AUC) indicated that the ensemble model accurately predicted the distribution of CP and LS (AUC > 0.8). Slope and clay content proved to be the most important factors affecting CP, whereas distance from faults and precipitation seasonality played more roles in LS susceptibility. The classification results indicated varying susceptibility levels to CP and LS in Khorasan-Razavi province, with approximately 31.58% categorized as low and 15.24% as very high LS susceptibility, while 42.71% were in the low CP susceptibility class. Overall, 57.16% of the area is safe from both hazards; however, 6.16% is vulnerable to both hazards, with more than 35% at risk for at least one hazard. Future prediction models suggest that up to approximately 4% of the area will consist susceptible to both hazards under both scenario emissions and less than 1% of the study area will reduce susceptibility for both studied hazards in future. The majority of regions that remain susceptible are in the southern province. These results guide for soil management to protect soil and water from the effects of humans and climate alternation in poor areas worldwide.

Keywords Natural hazards, Land subsidence, Collapsed pipe, Climate change, Ensemble model

Iran, characterized by arid and semi-arid regions, faces significant climate risks that threaten its environment, economy, and social stability. Its diverse geography, including deserts and mountains, heightens vulnerability to various climate-related issues, impacting water resources, agriculture, public health, and biodiversity. To tackle these challenges effectively, a coordinated and proactive approach is essential for achieving sustainability and resilience[1]. Moreover, LS and CP are wide-ranging hazards that are particularly common in semi-arid regions of Iran and exacerbated by human activities and climate change (CC). Land use changes, groundwater and hydrocarbon exploitation, and changes in temperature, precipitation, and vegetation may alter the patterns of natural hazards including LS and CP. Understanding the factors that make landforms and soils susceptible to erosion and subsidence introduces another level of uncertainty in the modeling. To enhance the realism of the algorithms, these variables should be selected based on geology, geomorphology, and landform evolution[2,3]. However, geologic and geomorphic datasets that bear on landform evolution are commonly unavailable; thus, in practice, more readily available bioclimatic data that provide insights into past, present, and future conditions are commonly utilized. Nevertheless, it is unclear whether these factors are adequate or truly optimal for accurately

[1]Department of Natural Resources and Environmental Engineering, College of Agriculture, Shiraz University, Shiraz, Iran. [2]Department of Soil Science, College of Agriculture, Shiraz University, Shiraz, Iran. [3]Department of Environment, Tourism, Science, and Innovation (DETSI), Queensland Government, Brisbane 4305, Australia. ✉email: hr.pourghasemi@shirazu.ac.ir; hamidreza.pourghasemi@yahoo.com

mapping soil landform patterns. Incorporating additional datasets can help reduce uncertainty and test the performance of predictors in erosional land surface modeling.

Erosional landform spatial modeling has emerged as an effective tool for evaluating landscapes affected by gullies, LS, and CP. Such modeling has been used to analyze and monitor the spread of plant species, plan and initiate conservation initiatives, predict the impacts of future climate change (CC), and assess the effects of human activities on the spatial patterns of landforms. Machine learning (ML) plays an increasingly important role in enhancing erosional landform spatial modeling and mapping, as it reveals patterns that may not be easily identifiable through traditional statistical methods[3,4]. Additionally, ML enables more accurate forecasts of future states given its ability to deal with complex nonlinear relationships among influencing variables and soil landforms. By selecting appropriate algorithms and tuning model parameters, ML can minimize bias and variability in data interpretation, thus ensuring the reliability and objectivity of the models. Previous studies employed different ML and deep learning algorithems to predict geomorphological hazard including landslide[5–7], LS[8–11], Gully erosion[12–14]. Some other study focused on the projecting effect of climate change on hazard susceptibility include flood[15–17], see level rize[18], drought[19], and soil erosion[20]. However, some uncertainty remains in using individual ML algorithms to predict locations susceptible to erosion, LS, CP, and other hazards[4,15]. To mitigate these uncertainties, researchers can develop, implement, and assess ensemble models for the spatial mapping of erosional landforms. These models typically employ weighted averaging, assigning weights based on predictive accuracy measures[21]. Predictions generated by ensemble models are generally regarded as more reliable than those produced by individual algorithms. Several other published studies have utilized portions of the Khorasan Razavi province dataset to detect LS and CP through various deep learning techniques (including CNN and ensemble CNN-RNN) and geophysical methods (including ground penetrating radar and electrical resistivity radar), focusing on pedological and topological variables[22–24].

In previous studies, the effect of climate change on the sensitivity to geomorphological hazards in CP and LS has not been examined; however, the current research aims to combine environmental assessment, climate modeling, machine learning, and practical recommendations for soil management in the context of global climate changes. This study examined the environmental factors influencing these issues and employed an ensemble forecasting approach to identify areas vulnerable to CP and LS. Utilizing future climate scenarios, we projected the spatial distributions of LS and CP through 2090, revealing critical patterns and risks. By employing multiple individual machine learning algorithms and their ensembles, we try to improve the estimation of landform dynamics under present and future climate conditions. The novelty of the present research lies in the identification and forecasting of future erosional landforms using an ensemble method.

Results

Multicollinearity of predictor variables

Of the 18 factors, 14 had "multicollinearity" problems, and were excluded from further modeling (Table 1). Linear correlation coefficients between the remaining 14 variable ranges. The minimum correlation value was − 0.0007 (TWI ~ distance from faults) and the maximum correlation value was 0.646 (PCQ – PWM) (Table 1).

Model validation and variable importaance

AUC analysis showed that the performances of the individual and ensemble models were excellent to fair (Table 2). RF and SVM were identified as the best models for LS and CP, respectively, and the final ensemble maps achieved an AUC value of 0.84 CP and 0.87 LS. Our analysis and predictions can be valuable for identifying regions that require immediate attention to remediate LS and CP, including targeted land use planning, groundwater management, and infrastructure location and design. Several key factors were identified in our comparative analysis of environmental variables using the best model (Fig. 1). For CP development, slope and clay content were the two most important variables, suggesting that areas with steeper slopes and proximity to

Variable	VIF	Tolerance	Unit
Aspect	1.00	0.963	-
Clay	1.35	0.648	%
Geology	1.31	0.644	-
Plan curvature	2.01	0.974	100/m
Elevation	2.85	0.300	meter
Fault density	1.44	0.529	km/km^2
Distance from Faults	1.58	0.556	meter
Distance from Rivers	1.08	0.893	meter
Slope	1.61	0.549	Angel
Silt	1.56	0.643	%
TWI	1.00	0.970	-
PWM	2.27	0.300	mm
PS	1.43	0.424	mm
PCQ	2.29	0.411	mm

Tabù. VIF results between independent variables.

Hazard	Models	Area	Standard error	Asymptotic significant	Asymptotic 95% confidence interval	
					Lower bound	Upper bound
LS	FDA	0.76	0.07	0.00	0.62	0.90
	Ensemble	0.84	0.05	0.00	0.74	0.95
	GLM	0.76	0.07	0.00	0.62	0.89
	Mars	0.71	0.07	0.01	0.57	0.86
	RF	0.84	0.05	0.00	0.74	0.95
	SVM	0.88	0.05	0.00	0.77	0.98
CP	FDA	0.79	0.05	0.00	0.69	0.89
	Ensemble	0.87	0.04	0.00	0.79	0.95
	GLM	0.77	0.05	0.00	0.66	0.88
	MARS	0.85	0.05	0.00	0.76	0.95
	RF	0.90	0.04	0.00	0.83	0.97
	SVM	0.87	0.04	0.00	0.79	0.95

Table 2. Area under the ROC curve.

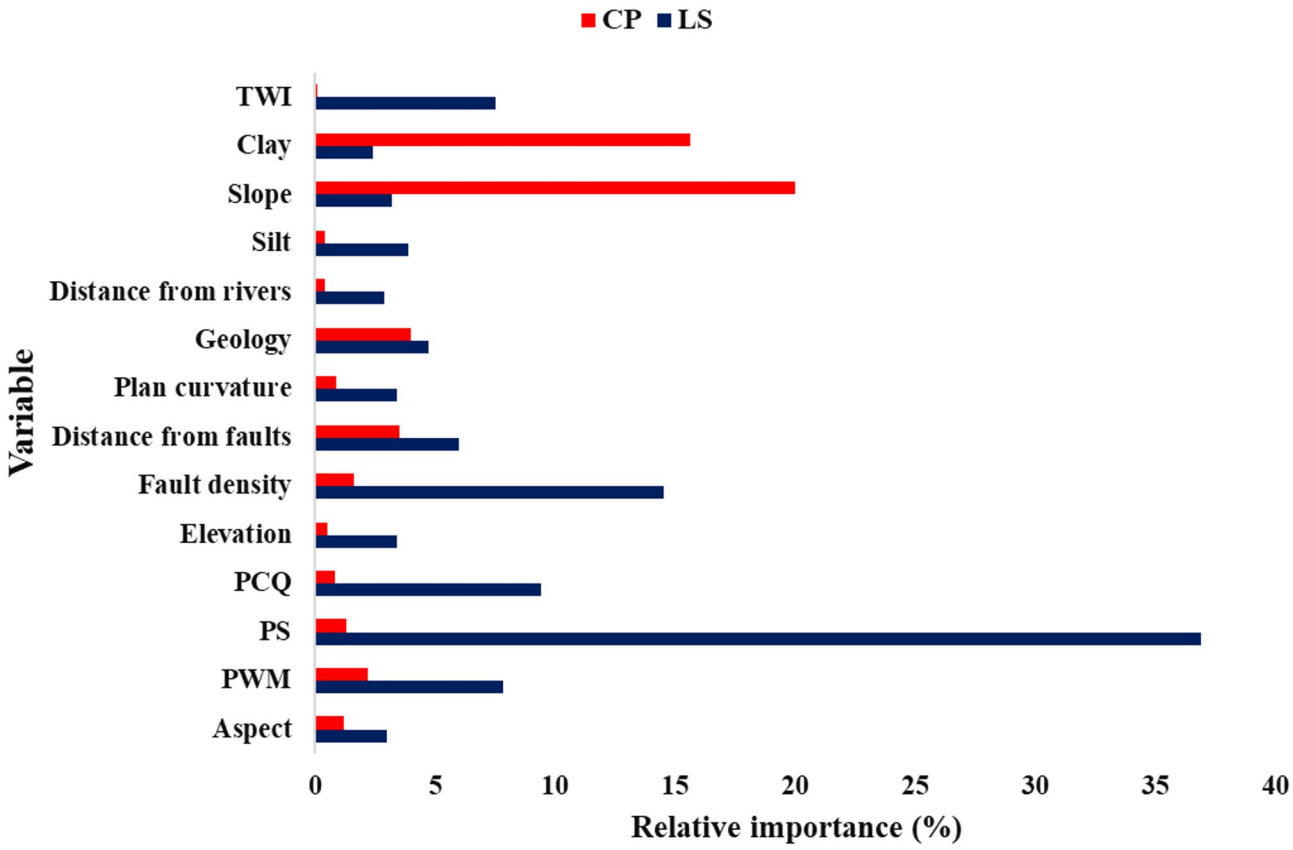

Fig. 1. Comparative analysis of variable importance metrics across the best model.

clay texture are prone to this hazard. Next to it, falt density and seasonal precipitation were identified as the most important LS, implying that areas adjacent to falts that experience greater seasonal amounts of precipitation are most susceptible to subsidence. In contrast, clay content was found to have the lowest relationship with subsidence, indicating that soil texture has a minimal influence on LS, and proximity to rivers has little significance in erosional processes.

Current and future susceptibility prediction of LS and CP using the ensemble model

The classification outputs show the regions that are most susceptible to LS and CP (Fig. 2). In the LS susceptibility map, approximately 31.58%, 27.51%, 25.67%, and 15.24% of the study region had low, medium, high, and very high susceptibility to land subsidence hazards, respectively. The CP map implied that 42.71% and 22.07% of the

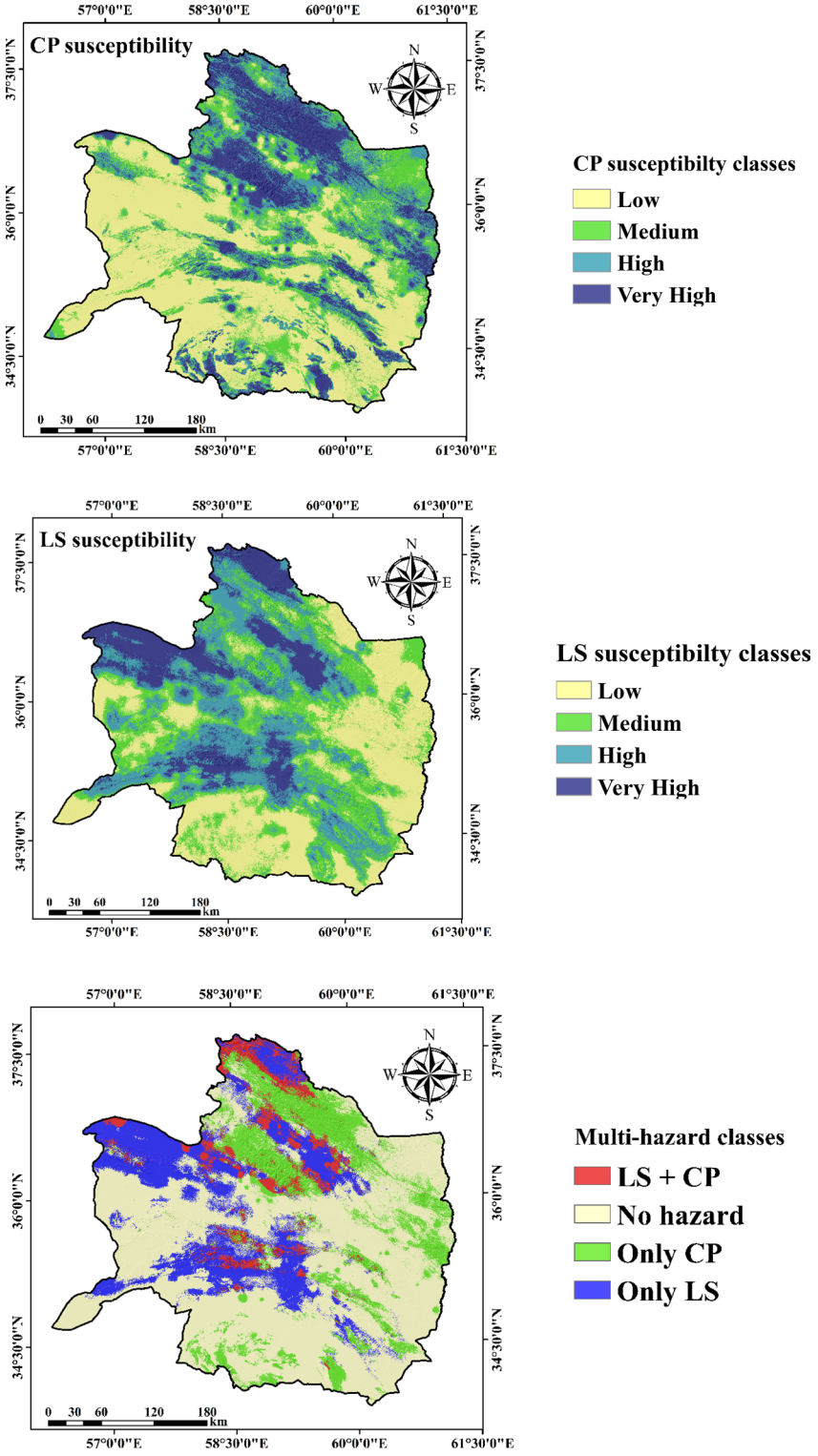

Fig. 2. Current soil landform susceptibility of LS and CP using Ensemble model.

province were in the low and medium susceptibility classes, respectively, and 17.33% and 17.89% of the region had high and very high susceptibility to CP, respectively. The results also indicate that 57.16% of the research sites were safe from the two studied hazards, whereas 6.16% of Khorasan-Razavi province was susceptible to both hazards. More than 35% of the region is susceptible to hazards. The future prediction model using the ensemble ML algorithm indicates that approximately 17% of the study area will never be LS to CP, but will be susceptible to LS in 2030 and 2050 for both low and high emission scenarios (Fig. 3) and will increase to about 50% under SSP 585 in 2070 and 2090. In addition, approximately 4% of the region will remain susceptible to

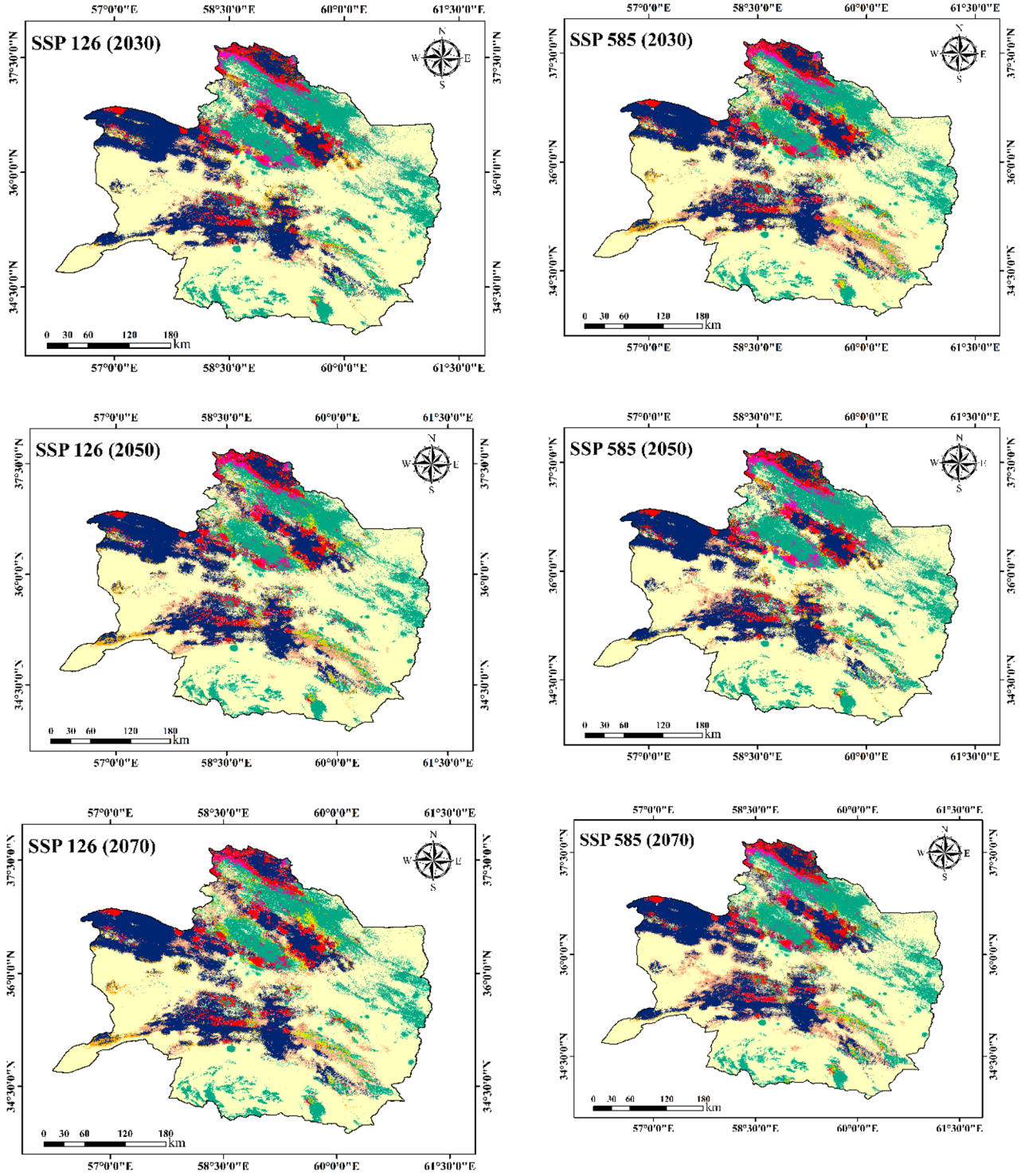

Fig. 3. Future projection of soil landforms according to the ensemble model.

both hazards, while approximately 1% and 3% of the study area will have increased susceptibility to CP and LS under both optimistic and pessimistic scenarios in the future, respectively. This modeling implies that the spatial distribution of LS and CP will be considerably affected by future CC (Fig. 4). Under the SSP 126 scenario, the values show relatively stable trends with minor fluctuations across the years. For inctance, the area where indicating a consistent pattern of low susceptibility for both hazards remains dominant (50–53%) from 2030 to 2090. Similarly, other areas where constantly not susceptible to CP and susceptible to LS and vice versa exhibit only slight variations, suggesting that the low emission scenario has a limited impact on altering susceptibility patterns over time.

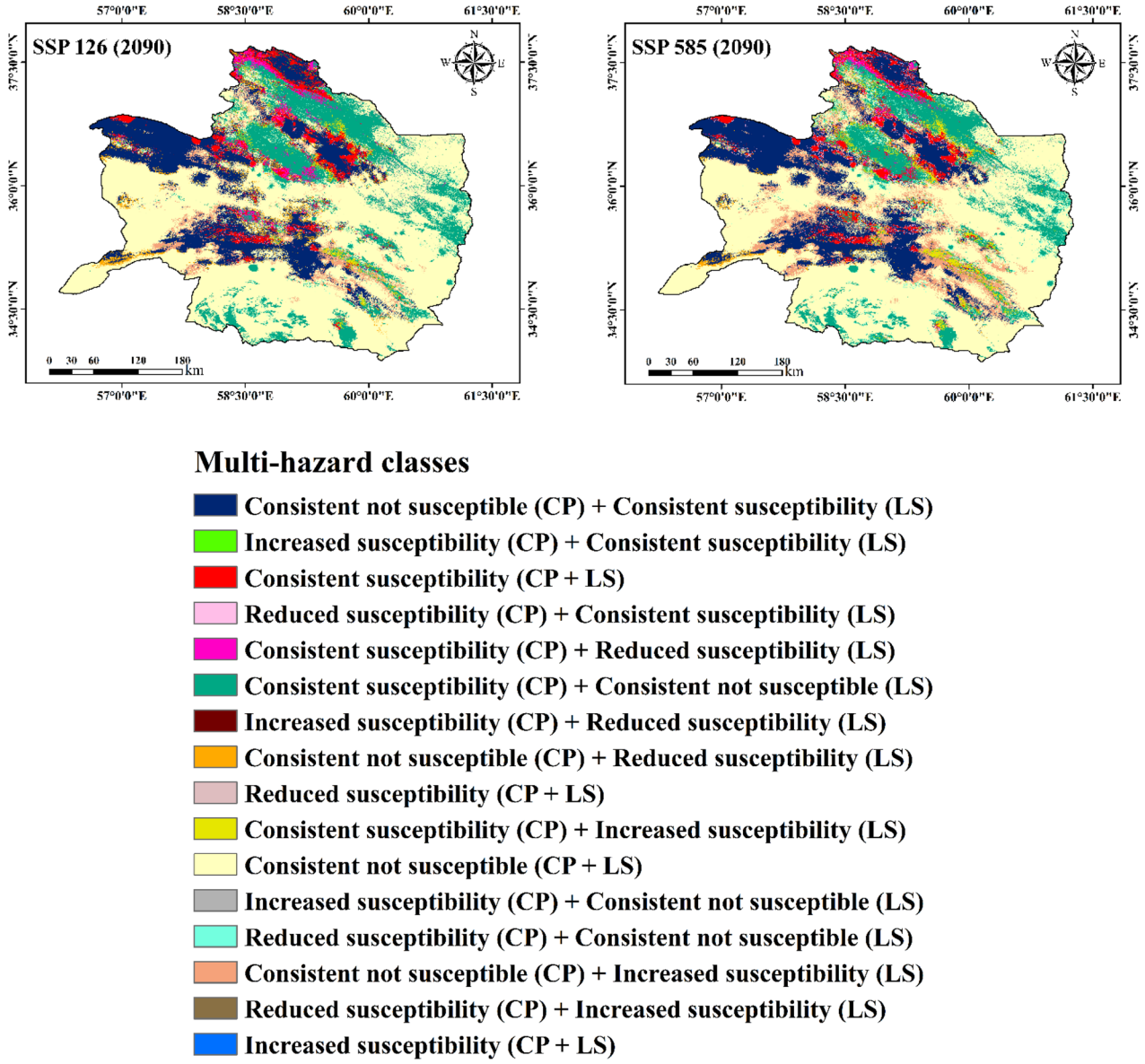

Fig. 3. (continued)

In contrast, the SSP 585 scenario reveals significant changes, particularly in the later years of 2070 and 2090. For example, the areas where consistently not susceptible to CP and susceptibility to LS experiences a dramatic increased, reaching 50.34% in 2070 and 48.76% in 2090, indicating a substantial shift in susceptibility patterns under high emissions. Conversely, the previously dominant areas where consistently not susceptible for both hazards drops to near 0% in the same years, underscoring the profound impact of high emissions on this class. Other regions, where consistent not susceptible to CP and increased susceptibility to LS, reduced susceptibility CP and consistent not susceptible LS, also show notable fluctuations, reflecting the heightened vulnerability and instability induced by the high emission scenario. These trends emphasize the critical need for emission reduction strategies to mitigate the adverse effects on susceptibility and consistency, ensuring a more stable and resilient future.

Discussion

LS and CP are challenging erosional processes in Iran with significant implications because of their profound impacts on agriculture and other land uses. The current study found that slope is the most significant factor affecting the distribution of CP in Khorasan-Razavi province. Additionally, precipitation is positively linked to subsidence-prone areas; areas with heavy winter rainfall are more prone to this hazard than are other areas. However, the historic decrease in rainfall in the province has resulted in drought conditions, higher temperatures, and depletion of groundwater and surface water. The increased exploitation of groundwater has exacerbated LS in many parts of the province. The findings of emission pathway modeling on the occurrence of LS and CP highlight the potential differences in the future trajectories of both hazard and non-hazard areas.

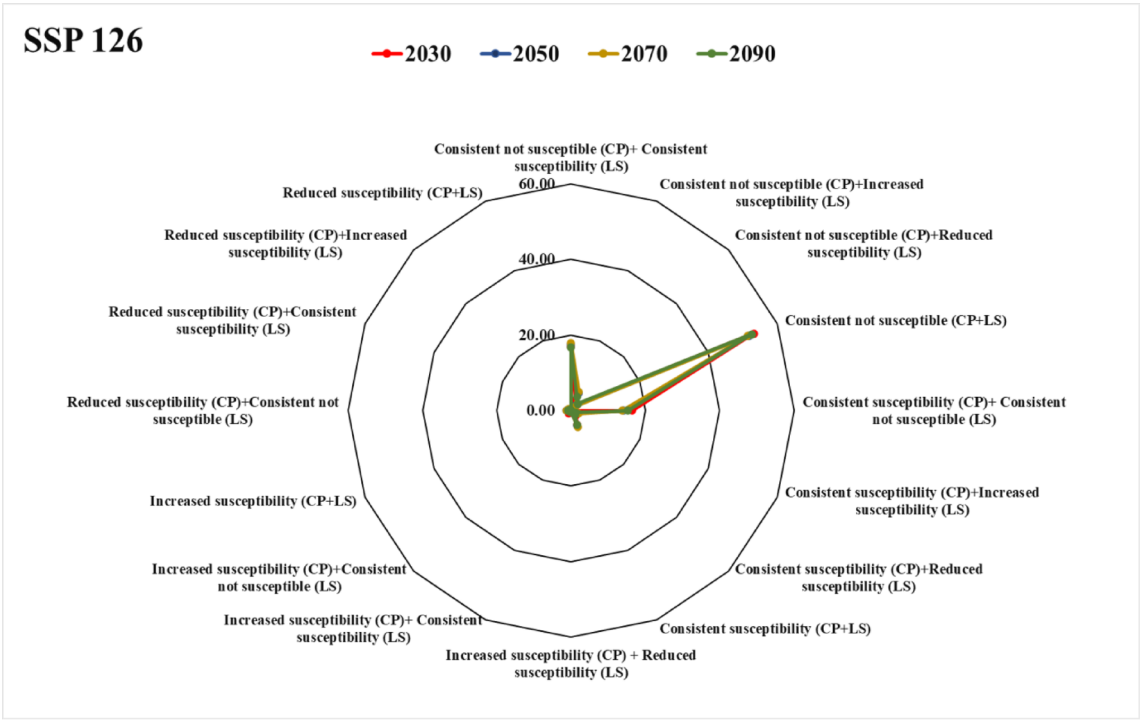

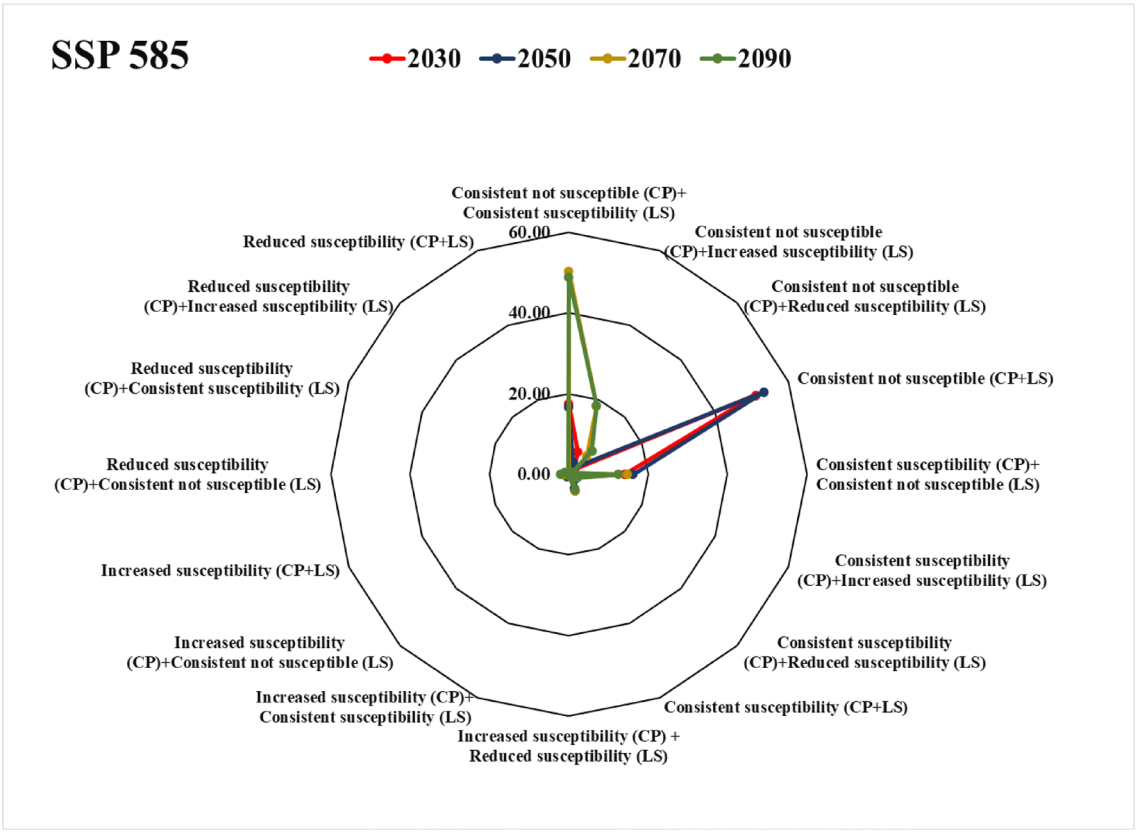

Fig. 4. The percentage of the multi-hazards future projection of soil landforms according to the ensemble model.

The results indicate that under the lowest emission pathway, a higher proportion of the study area maintained its non-hazard status for a longer period. In contrast, under the highest emissions scenario, non-hazardous areas are projected to decline slightly by 2090. Understanding these temporal trends can inform decision making related to infrastructure development, land-use planning, and risk reduction strategies. This study highlights the importance of climatic, terrain, and other factors in controlling these processes. We found that the RF model is effective in identifying the most important factors controlling CP hazards in Khorasan-Razavi province. The RF, which is widely used for evaluating variable importance, is a flexible machine-learning algorithm capable of processing large datasets and capturing complex interactions between landforms and their environments. Previous research has demonstrated the suitability of RF for predicting the spatial distribution of soil landforms[25]. As stated by Ebrahimi, et al.[26], the ongoing challenges posed by CC necessitate proactive measures that address the complexities of ecological interactions, reinforcing the imperative for adaptive management approaches rooted in latest scientific advancements.

In our study, the use of climate data for modeling erosional landforms using the ensemble model indicated that global warming may increase soil erosion vulnerability. Janizadeh, et al.[3] predicted flood-susceptibility under CC scenarios using three ML algorithms, including CIRF, KKN, and RRF. They examined the effects of two scenarios, SSP1-2.6, and SSP5-8.5, on future flood risk during 2041–2060 and 2081–2100. Their results showed that machine-learning models were effective in modeling flood susceptibility.

The results from the classification of land susceptibility to LS and CP provide critical insights into the geohazards facing Khorasan-Razavi province. The data indicate that although a significant portion of the study region (approximately 57.16%) is currently safe from these hazards, a substantial fraction (over 35%) is susceptible to at least one of the hazards. This susceptibility can have profound implications for landuse planning, infrastructure development, and environmental management. The susceptibility map for LS revealed a concerning distribution of risk: 31.58% of the area was classified as low susceptibility, while medium, high, and very high susceptibility zones collectively accounted for a considerable portion of the region. In contrast, the CP map shows that approximately 42.71% of the region falls into the low susceptibility category, but still highlights that 35.22% is exposed to very high and high levels of risk. These statistics suggest an urgent need for targeted risk-mitigation strategies, especially in regions designated as very high and high susceptibility to either hazard. Predictive modeling employing ensemble ML algorithms indicates a worrying trend; it foresees a significant increase in susceptibility to LS over the next few decades, particularly under high-emission scenarios. The assertion that approximately 50% of the area could become susceptible to LS by 2070 under high emissions illustrates that CC is likely to exacerbate existing vulnerabilities. This aligns with broader research indicating that climate-related factors, such as increased precipitation variability and temperature changes, can affect subsurface water movements and soil properties, thereby enhancing the risk of LS and CP. Similar to our research, Roy, et al.[15] examined the influeence of CC and extreme rainfall on land resources in a subtropical monsoon region, focusing on gully susceptibility using ANN, SVM, DLNN, and ensemble Global Circulation Models to project rainfall scenarios for 2100 s. Their analysis showed that the DLNN provided the best predictive performance and highlighted an increasing trend in rainfall and gully erosion susceptibility, offering critical insights for long-term regional planning and decision making.

Notably, future predictions show that 4% of the region is projected to remain susceptible to both hazards, whereas approximately 1% and 3% are expected to show increased susceptibility to CP and LS, respectively. This indicates not only the persistence of current hazards but also an increase in risk profiles for these areas. The identified regions, particularly the southern part of the province, which are expected to remain highly susceptible, underscore the need for detailed risk assessments and adaptation strategies tailored to local conditions. The analysis further revealed valuable information regarding the effectiveness of climate-change mitigation efforts. Under low-emission scenarios, 57% of the province is expected to remain safe from LS and CP by 2070, compared to 55% under high-emission scenarios in 2090. These figures highlight the importance of adopting aggressive emission-reduction strategies to curb CC and safeguard against geohazards. In line with our research, Saha, et al.[4] assessed future degradation-risk dynamics through the Coupled Model Intercomparison Project six down-scale-based ensembles of nine global climate models in four SSPs scenarios. They implied that the combination of climate modeling and deep learning should be helpful for enhancing the results more precisely. The research was published by Heo, et al.[27] employed a machine learning model to assess the geographic susceptibility of natural hazard risks on Kalimantan Island, Indonesia. It found that mountainous and island regions are particularly vulnerable, highlighting the importance for decision-makers to pinpoint high-risk areas. The study reported a predicted risk of 22.6% for drought and 21.7% for forest fires, with 2.6% of locations at risk for both. Risks are anticipated to increase under two climate scenarios (RCP-SSP2-4.5 and RCP-SSP5-8.5), with West Kalimantan showing the highest forest fire risk (33.02%) and South Kalimantan the highest drought risk (67.3%). The worst-case scenario projects even greater risks, mainly due to climate change and heat waves, necessitating a revision of past risk management strategies. The Random Forest model used in the study provided reliable forecasts, offering important insights for future hazard management efforts.

In summary, this study serves as a call to action, underscoring the imperatives for immediate research, responsive policy frameworks, and community engagement in soil management to safeguard against threats posed by LS and CP. By prioritizing these efforts, regions at risk can better protect their natural resources while fostering resilient communities capable of adapting to the challenges of CC. The limitation and future research direction is that this study examined the effect of CC on multi-geomorhphologic hazards. Although climatic factors affect these hazards, groundwater, over-exploitation, and the subsequent decline in aquifer levels are key contributors to these geomorphological hazards. Future researchers should assess changes in aquifer levels and underground water usage by employing mathematical models within the context of CC scenarios. This information should be used as a significant and influential factor in future studies. Moreover, the present study on the impact of climate change on geomorphological hazards, specifically LS and CP, in Khorasan-Razavi

province, Iran, has significant implications for both regional and global contexts. In the regional context, the study highlights that LS and CP pose significant environmental and socio-economic threats, particularly in arid and semi-arid regions like Khorasan-Razavi province. These hazards can lead to infrastructure damage, loss of agricultural productivity, and displacement of communities, exacerbating poverty and resource scarcity in already vulnerable areas. Moreover, the findings provide a scientific basis for local governments and policymakers to implement targeted land management strategies. For instance, areas identified as highly susceptible to LS and CP could be prioritized for conservation efforts, land-use restrictions, or engineering interventions to mitigate risks. Also, since LS and CP are influenced by hydrological factors, the study underscores the need for improved water resource management. Over-extraction of groundwater, a common issue in arid regions, can exacerbate LS. Policies promoting sustainable water use and recharge practices are critical.

In the global contexts, the study's methodology and findings are applicable to other arid and semi-arid regions worldwide facing similar geomorphological hazards. Regions in Africa, the Middle East, Central Asia, and parts of the Americas could benefit from similar assessments to adapt to climate change impacts. Also, The ensemble forecasting approach used in this study can serve as a model for predicting and mitigating LS and CP in other regions. By identifying key factors such as slope, clay content, distance from fults, and precipitation seasonality, other regions can develop tailored risk mitigation strategies. In addition, addressing LS and CP aligns with several SDGs, including SDG 13 (Climate Action), SDG 15 (Life on Land), and SDG 6 (Clean Water and Sanitation). The study's emphasis on protecting soil and water resources contributes to global efforts to achieve these goals. Further, the present study not only addresses the specific challenges of LS and CP in Khorasan-Razavi province but also offers a scalable and adaptable framework for addressing similar hazards globally. Its interdisciplinary approach, emphasis on climate change scenarios, and focus on vulnerable regions make it a valuable contribution to the fields of geomorphology, climate science, and sustainable development. By integrating these findings into policy and practice, stakeholders can better prepare for and mitigate the impacts of climate change on geomorphological hazards.

Our study underscores the critical importance of understanding the susceptibility of LS and CP in the Khorasan-Razavi province. The patterns revealed by our ensemble modeling approach not only highlight current vulnerabilities but also project future risks, emphasizing the urgent need for effective land management strategies and emission reduction initiatives. Addressing these issues will be essential for ensuring the resilience of the region against the adverse impacts of climate change and land degradation. Despite the valuable insights provided by this study, several limitations should be acknowledged. One significant limitation is the issue of multicollinearity among predictor variables, where 7 out of 21 variables exhibited multicollinearity problems and were consequently excluded from further modeling. This exclusion may have led to an oversimplification of the relationships among environmental factors influencing LS and CP, potentially omitting important interactions that could refine model accuracy. Additionally, while the study utilized advanced machine learning models, the performance metrics, although showing good results, may not capture the full complexity of real-world scenarios due to the inherent uncertainties in predicting future conditions based on historical data. Moreover, the focus on specific geographic regions limits the generalizability of the findings; variations in local geology, climate, and land use practices may yield different susceptibility patterns elsewhere. Future research should consider integrating a broader range of variables and models, as well as validating predictions against real-world observations to enhance the robustness of findings. Lastly, the predictions regarding future susceptibility to LS and CP under different emission scenarios are contingent upon the accuracy of climate models and socio-economic projections, which can be inherently uncertain. Thus, while the study presents a comprehensive analysis, the aforementioned limitations warrant careful consideration when interpreting results and formulating land management strategies.

Materials and methods

The conceptual framework employed in this study is illustrated in Fig. 5. It involves several steps: (1) mapping the locations of sites affected by LS and CP, (2) preparation of training and testing datasets, (3) choosing possible climatic and environmental variables for modeling and performing a multicollinearity analysis, (4) spatial modeling of current areas affected by LS and CP and their multi-hazard, followed by a validation assessment, and (5) projecting future changes in hazard susceptibility.

Study area

In northeastern Iran, Khorasan-Razavi province is between 55°E and 61°E longitude and 30°N and 38°N latitude (Fig. 6). It is a semiarid region covering an area of 298,481 km^2[22]. Its agricultural sector, operating on 10% of Iran's total cultivated area and accounting for 9% of its irrigated wheat production, is crucial to'san the national economy. The average annual rainfall-AAR in the province ranges from approximately 300 to 400 mm; however, the amount of rainfall in the eastern, southern, and central regions is lower (approximately 150 mm).

Geomorphological hazards are particularly prominent in Khorasan-Razavi province due to several interrelated factors. The combination of geological, climatic, and anthropogenic factors makes Khorasan-Razavi province particularly vulnerable to geomorphological hazards, necessitating continued research and monitoring to mitigate their impacts[28].

Documenting LS and CP in the study area

We identified 201 LS and CP sites in Khorasan-Razavi province based on scientific reports, extensive field surveys, and data provided by the province's natural resources and watershed management organization (https://en.frw.ir/). These sites included 82 LS and 119 CP sites. We then randomly chose an equal number of hazard and no-hazard sites to perform spatial modeling[29,30], and placed them in training (70%) and testing (30%) datasets[31,32].

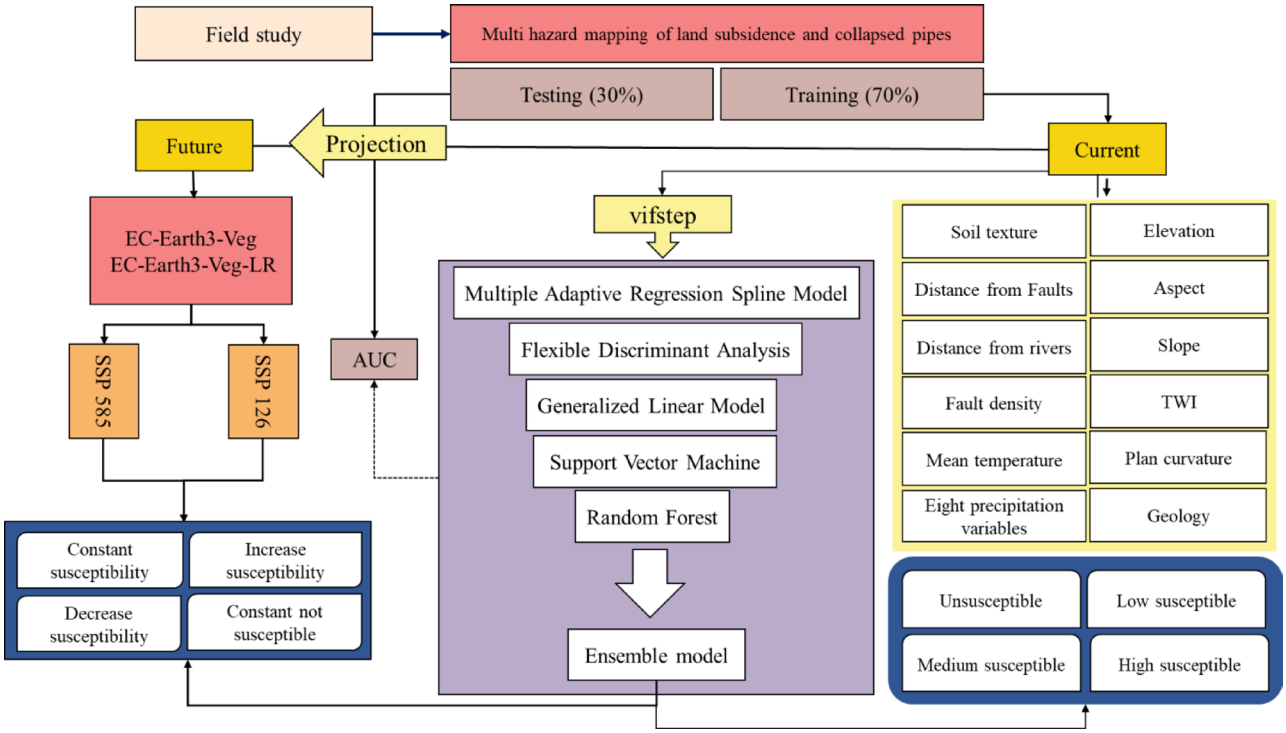

Fig. 5. Outline of the methodology.

Independent data Preparation

Climate data

Climate data with 30-second spatial resolution for the period 1970–2000 were acquired from the "WorldClim" data-base ("http://www.worldclim.org")[33]. We used a variety of precipitation and temperature data for modeling (Table 3).

Geo-environmental variables

According to a review of the existing literature and expert knowledge, we selected the primary factors that impact both LS and CP. These factors were grouped into four categories: geology (lithology, distance from fults, and fault density)[32,34], topography ("slope angle, slope aspect, elevation, and plan curvature")[35,36], hydrology (distance from rivers and topographic wetness index)[37], and edaphic (soil texture)[25]. Terrain variables were measured using "Shutter Radar Topography Mission (SRTM)" DEM with 90 M resolution. These layers were generated applying "SAGA-GIS" software[38], and "ArcGIS" v.10.4.1 ("https://www.esri.com").

Pre-selection and multicollinearity analysis

All quantitative variables were clipped to the study region and downscaled to a 50 m resolution using the nearest-neighbor technique. To avoid overfitting and enhance transferability, we chose only the most significant variables[39]. To this end, we used a stepwise approach (vifstep) and Tollerance (TOL) implemented in the SPSS software (version 26). The vifstep function automatically eliminates collinear variables sequentially until the "Variance Inflation Factor" (VIF) of all remaining quantitative variables is below a threshold value of 10 [40].

Application of ML algorithms

We applied five widely used ML algorithms to establish a multi-hazard assessment in the Khorasan-Razavi province: random forest (RF)[41], generalized linear model (GLM)[42], support vector machine (SVM)[43], flexible discriminant analysis (FDA)[44,] and multiple adaptive regression spline (MARS)[45]. We effectively addressed the potential limitations and biases inherent in specific models by applying this broad range of modeling techniques[26].

Next, we employed an ensemble technique to merge the susceptibility maps created with the individual models applying the weighted average method. Individual ML methods typically generate noise along with the signals[46]. The purpose of ensembles is to combine models to improve the separation of signals from noise[47,48] and reduce the uncertainty resulting from the use of single models[49]. To enrich the hazard susceptibility map in the study, we applied training data, selected variables, and created an ensemble model in the SDM package[50] using "R statistical software 4.0.3" (R Development Core Team, 2021). To facilitate understanding of the outcomes, hazard levels were binned into four groups based on the natural break classification method. To enhance the interpretation of the results, we categorize the predicted map into four classes using the Jenks natural breaks classification method[51].

To determine the accuracy of the final model, we used AUC, which is a threshold-independent analysis[9]. The AUC is a widely used metric to determine the ability of a model to correctly classify hazards (ranging from 0

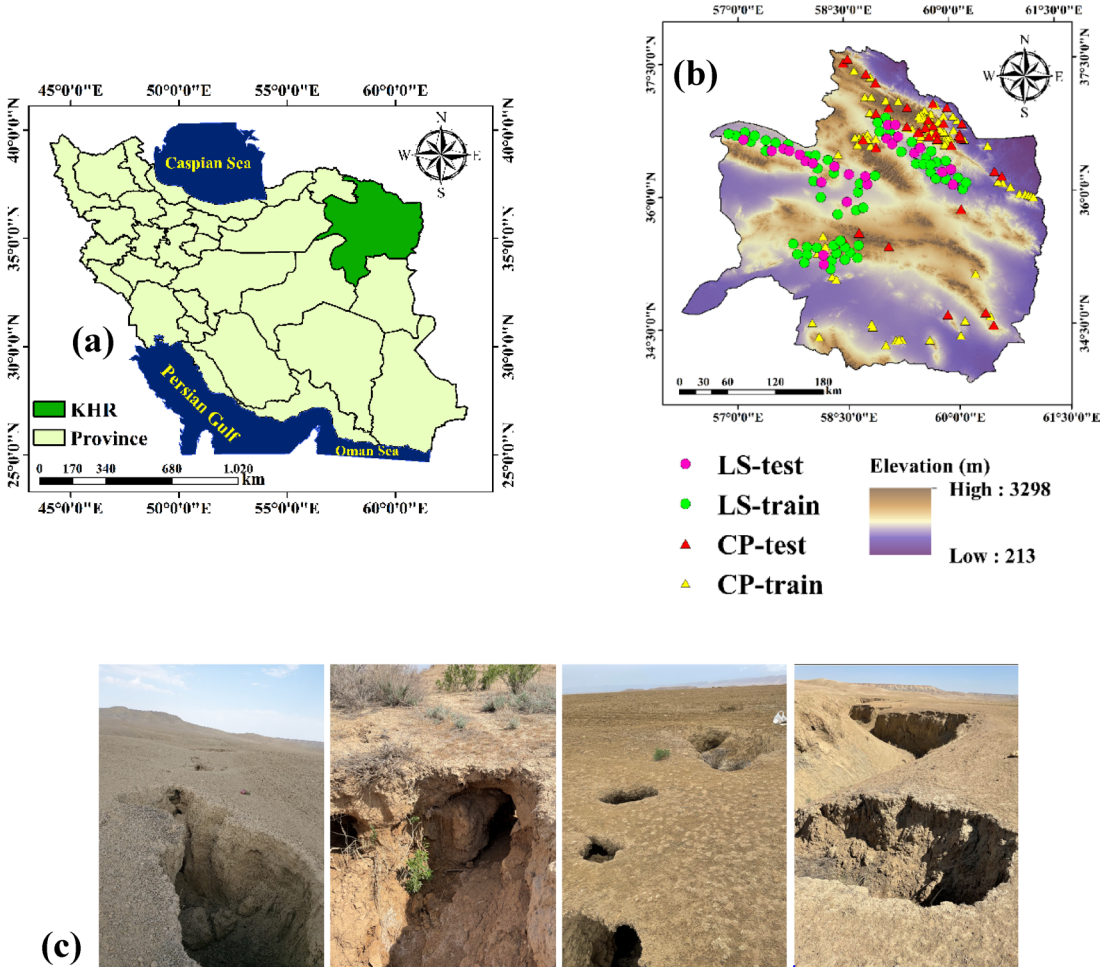

Fig. 6. Location and details of the study area: a) Iran, b) Khorasan Razavi province, c) Sample erosional landforms (Photo by Narges Kariminejad, 2022).

Abbreviation	Description	Unit
AMT	Annual Mean Temperature	°C
AP	Annual Precipitation	mm
PWM	Precipitation of Wettest Month	mm
PDM	Precipitation of Driest Month	mm
PS	Precipitation Seasonality	-
PWQ	Precipitation of Wettest Quarter	mm
PDQ	Precipitation of Driest Quarter	mm
PWQ	Precipitation of Warmest Quarter	mm
PCQ	Precipitation of Coldest Quarter	mm

Table 3. Climate variables used in the present study.

to 1). Values of 1 and 0.5 indicate, respectively, perfect and random discrimination, respectively[52]. We assigned AUC values as follows: "fail (0.5–0.6), poor (0.6–0.7), fair (0.7–0.8), good (0.8–0.9), and excellent (0.9–1.0)"[53,54].

Future multi-hazard projection

Estimates of areas of future LS and CP in the study area were based on climate forecasts of the "Coupled Model Intercomparison Project Phase 6 (CMIP6)". We chose two climate pathways (low emissions: "SSP 1–2.6" and High emissions: "SSP 5–8.5") and based on two global circulation models (GCMs, Table 4) for the years 2030 (2021–2040), 2050 (2041–2060), 2070 (2061–2080), and 2090 (2081–2100).

A binary map (hazard and non-hazard) was created by converting the continuous potential susceptibility map using a threshold determined through a threshold optimization technique that maximizes the "sensitivity"

GCM	Institution, country	Resolution
EC-Earth3-Veg	EC-Earth-Consortium, Europe	0.70°×0.70°
EC-Earth3-Veg-LR	EC-Earth-Consortium, Europe	0.70°×0.70°

Table 4. Detailed description of the selected GCMs.

and "specificity statistics"[50]. Considering the binary maps for the current and future periods resulted in the classification of pixels into four categories: (1) consistent susceptibility, (2) reduced susceptibility, (3) increased susceptibility, and (4) consistent susceptibility[55].

Conclusion

This study provides crucial insights into the interplay between climate change and geomorphological hazards, specifically LS and CP, in Khorasan-Razavi province, Iran. By implementing an ensemble forecasting approach, we have successfully pinpointed areas vulnerable to these hazards under both current and projected future climate scenarios. Our findings reveal that key factors influencing susceptibility include slope and clay content for CP, and distance from faults, and precipitation seasonality for LS. Notably, while 57.16% of the region currently remains safe from both hazards, a concerning 6.16% faces dual risks, with over 35% exposed to at least one type of hazard. Projections for the future indicate a dramatic rise in susceptibility, especially under high-emission scenarios (SSP 5–8.5), suggesting that by 2070, nearly half of the region may be at risk for LS, particularly in southern hotspots.

The novelty of this study lies in its application of ensemble machine learning models to enhance CP and LS prediction, providing a framework that can inform effective land-use planning and sustainable groundwater management strategies. These insights are vital for policymakers and stakeholders as they develop proactive responses to mitigate the impacts of climate change. Future research should build on these findings by integrating groundwater dynamics and trends in aquifer depletion to deepen our understanding of geomorphological hazards and their drivers in a changing climate.

Data availability

Data will be sent based on request by corresponding author.

Received: 24 February 2025; Accepted: 19 May 2025
Published online: 26 May 2025

References

1. Sadeghi, S. H. & Hazbavi, Z. *In Global Degradation of Soil and Water Resources: Regional Assessment and Strategies*287–314 (Springer, 2022).
2. Saupe, E. E. et al. Variation in niche and distribution model performance: the need for a priori assessment of key causal factors. *Ecol. Model.* **237**, 11–22 (2012).
3. Janizadeh, S. et al. Impact of climate change on future flood susceptibility projections under shared socioeconomic pathway scenarios in South Asia using artificial intelligence algorithms. *J. Environ. Manage.* **366**, 121764 (2024).
4. Saha, A. et al. Threats of soil erosion under CMIP6 SSPs scenarios: an integrated data mining techniques and Geospatial approaches. *Geocarto Int.* **37**, 17307–17339 (2022).
5. Merghadi, A. et al. Machine learning methods for landslide susceptibility studies: A comparative overview of algorithm performance. *Earth Sci. Rev.* **207**, 103225 (2020).
6. Azarafza, M., Azarafza, M., Akgün, H., Atkinson, P. M. & Derakhshani, R. Deep learning-based landslide susceptibility mapping. *Sci. Rep.* **11**, 24112 (2021).
7. Tehrani, F. S., Calvello, M., Liu, Z., Zhang, L. & Lacasse, S. Machine learning and landslide studies: recent advances and applications. *Nat. Hazards*. **114**, 1197–1245 (2022).
8. Tien Bui, D. et al. Land subsidence susceptibility mapping in South Korea using machine learning algorithms. *Sensors* **18**, 2464 (2018).
9. Rahmati, O. et al. Land subsidence modelling using tree-based machine learning algorithms. *Sci. Total Environ.* **672**, 239–252 (2019).
10. Li, H. et al. Spatiotemporal modeling of land subsidence using a geographically weighted deep learning method based on PS-InSAR. *Sci. Total Environ.* **799**, 149244 (2021).
11. Kariminejad, N. et al. Evaluation of various deep learning algorithms for landslide and sinkhole detection from UAV imagery in a semi-arid environment. *Earth Syst. Environ.* **8**, 1387–1398 (2024).
12. Arabameri, A. et al. Comparison of machine learning models for gully erosion susceptibility mapping. *Geosci. Front.* **11**, 1609–1620 (2020).
13. Chen, W. et al. Evaluation of different boosting ensemble machine learning models and novel deep learning and boosting framework for head-cut gully erosion susceptibility. *J. Environ. Manage.* **284**, 112015 (2021).
14. Huang, D., Su, L., Fan, H., Zhou, L. & Tian, Y. Identification of topographic factors for gully erosion susceptibility and their Spatial modelling using machine learning in the black soil region of Northeast China. *Ecol. Ind.* **143**, 109376 (2022).
15. Roy, P. et al. Evaluation of climate change impacts on future gully erosion using deep learning and soft computational approaches. *Geocarto Int.* **37**, 12709–12745 (2022).
16. Pal, S. C. et al. Threats of climate change and land use patterns enhance the susceptibility of future floods in India. *J. Environ. Manage.* **305**, 114317 (2022).
17. Chakrabortty, R. et al. Impact of climate change on future flood susceptibility: an evaluation based on deep learning algorithms and GCM model. *Water Resour. Manage.* **35**, 4251–4274 (2021).
18. Roy, P. et al. Effects of climate change and sea-level rise on coastal habitat: vulnerability assessment, adaptation strategies and policy recommendations. *J. Environ. Manage.* **330**, 117187 (2023).
19. Roy, P. et al. Climate change and groundwater overdraft impacts on agricultural drought in India: vulnerability assessment, food security measures and policy recommendation. *Sci. Total Environ.* **849**, 157850 (2022).

20. Pal, S. C. & Chakrabortty, R. *Climate Change Impact on Soil Erosion in Sub-tropical Environment: Application of Empirical and Semi-empirical Models* (Springer Nature, 2022).
21. Wang, D. et al. Global assessment of the distribution and conservation status of a key medicinal plant (Artemisia annua L.): the roles of climate and anthropogenic activities. *Sci. Total Environ.* **821**, 153378 (2022).
22. Kariminejad, N. et al. Detection of land subsidence using hybrid and ensemble deep learning models. *Appl. Geomatics*. **16**, 593–610 (2024).
23. Kariminejad, N., Sepehr, A., Garajeh, M. K., Ahmadi, A. & Gholamhosseinian, A. Deep learning-based predictive models of land subsidence and collapsed pipes in Razavi Khorasan Province, Iran. *Earth Sci. Inf.* **17**, 3529–3545 (2024).
24. Kariminejad, N., Sepehr, A., Poesen, J. & Hassanli, A. Combining UAV remote sensing and pedological analyses to better understand soil piping erosion. *Geoderma* **429**, 116267 (2023).
25. Kariminejad, N., Pourghasemi, H. R. & Hosseinalizadeh, M. Analytical techniques for mapping multi-hazard with geo-environmental modeling approaches and UAV images. *Sci. Rep.* **12**, 14946 (2022).
26. Ebrahimi, E., Araújo, M. B. & Naimi, B. Flood susceptibility mapping to improve models of species distributions. *Ecol. Ind.* **157**, 111250 (2023).
27. Heo, S., Park, S. & Lee, D. K. Multi-hazard exposure mapping under climate crisis using random forest algorithm for the Kalimantan Islands, Indonesia. *Sci. Rep.* **13**, 13472 (2023).
28. Mohamadkhan, S., Namjooyan, R., Barzkar, M. & Abbasi, M. The evaluation of geomorphologic landforms for the development of human settlements: A case study of Southeast cities of Razavi Khorasan Province. *Town Ctry. Plann.* **13**, 167–191 (2021).
29. Zhao, D. et al. Comparative performance assessment of landslide susceptibility models with presence-only, presence-absence, and pseudo-absence data. *J. Mt. Sci.* **17**, 2961–2981 (2020).
30. Mobley, W. & Blessing, R. in *Coastal Flood Risk Reduction* 61–75Elsevier, (2022).
31. Bausilio, G. et al. *In Geotechnical Engineering for the Preservation of Monuments and Historic Sites III*1112–1123 (CRC, 2022).
32. Bianchini, S. et al. Machine learning for sinkhole risk mapping in Guidonia-Bagni Di tivoli plain (Rome), Italy. *Geocarto Int.* **37**, 16687–16715 (2022).
33. Fick, S. E. & Hijmans, R. J. WorldClim 2: new 1-km Spatial resolution climate surfaces for global land areas. *Int. J. Climatol.* **37**, 4302–4315 (2017).
34. Pradhan, B., Abokharima, M. H., Jebur, M. N. & Tehrany, M. S. Land subsidence susceptibility mapping at Kinta Valley (Malaysia) using the evidential belief function model in GIS. *Nat. Hazards*. **73**, 1019–1042 (2014).
35. Rahmani, P., Gholami, H. & Golzari, S. An interpretable deep learning model to map land subsidence hazard. *Environ. Sci. Pollut. Res.* **31**, 17448–17460 (2024).
36. Ramírez-Serrato, N. L., García-Cruzado, S., Herrera, G., Yépez-Rincón, F. & Villarreal, S. Assessing the relationship between contributing factors and sinkhole occurrence in Mexico City. *Geomatics Nat. Hazards Risk*. **15**, 2296377 (2024).
37. Yang, X., Jia, C., Sun, H., Yang, T. & Yao, Y. Integrating multi-source data to assess land subsidence sensitivity and management policies. *Environ. Impact Assess. Rev.* **104**, 107315 (2024).
38. Conrad, O. et al. System for automated geoscientific analyses (SAGA) V. 2.1. 4. *Geosci. Model Dev.* **8**, 1991–2007 (2015).
39. Dakhil, M. A., El-Barougy, R. F., El-Keblawy, A. & Farahat, E. A. Clay and Climatic variability explain the global potential distribution of Juniperus phoenicea toward restoration planning. *Sci. Rep.* **12**, 13199 (2022).
40. Feld, C. K., Segurado, P. & Gutierrez-Canovas, C. Analysing the impact of multiple stressors in aquatic biomonitoring data: A 'cookbook'with applications in R. *Sci. Total Environ.* **573**, 1320–1339 (2016).
41. Breiman, L. Random forests. *Mach. Learn.* **45**, 5–32 (2001).
42. Nelder, J. A. & Wedderburn, R. W. Generalized linear models. *J. Royal Stat. Soc. Ser. A: Stat. Soc.* **135**, 370–384 (1972).
43. Vapnik, V. N. An overview of statistical learning theory. *IEEE Trans. Neural Networks*. **10**, 988–999 (1999).
44. Hastie, T., Tibshirani, R. & Buja, A. Flexible discriminant analysis by optimal scoring. *J. Am. Stat. Assoc.* **89**, 1255–1270 (1994).
45. Friedman, J. H. Multivariate adaptive regression splines. *Annals Stat.* **19**, 1–67 (1991).
46. Hao, T., Elith, J., Guillera-Arroita, G. & Lahoz-Monfort, J. J. A review of evidence about use and performance of species distribution modelling ensembles like BIOMOD. *Divers. Distrib.* **25**, 839–852 (2019).
47. Araújo, M. B. & New, M. Ensemble forecasting of species distributions. *Trends Ecol. Evol.* **22**, 42–47 (2007).
48. Dormann, C. F. et al. Model averaging in ecology: A review of bayesian, information-theoretic, and tactical approaches for predictive inference. *Ecol. Monogr.* **88**, 485–504 (2018).
49. Thuiller, W., Lafourcade, B., Engler, R. & Araújo, M. B. BIOMOD–a platform for ensemble forecasting of species distributions. *Ecography* **32**, 369–373 (2009).
50. Naimi, B. & Araújo, M. B. Sdm: a reproducible and extensible R platform for species distribution modelling. *Ecography* **39**, 368–375 (2016).
51. Jenks, G. F. Generalization in statistical mapping. *Ann. Assoc. Am. Geogr.* **53**, 15–26 (1963).
52. Satarzadeh, E., Sarraf, A., Hajikandi, H. & Sadeghian, M. S. Flood hazard mapping in Western Iran: assessment of deep learning vis-à-vis machine learning models. *Natural Hazards*, 1–19 (2022).
53. Swets, J. A. Measuring the accuracy of diagnostic systems. *Science* **240**, 1285–1293 (1988).
54. Sahana, M. & Patel, P. P. A comparison of frequency ratio and fuzzy logic models for flood susceptibility assessment of the lower Kosi river basin in India. *Environ. Earth Sci.* **78**, 1–27 (2019).
55. Amindin, A. et al. Predicting current and future habitat suitability of an endemic species using data-fusion approach: responses to climate change. *Rangel. Ecol. Manage.* **94**, 149–162 (2024).

Acknowledgements

This project has been funded by the Office of Science and Technology Interactions, Research and Technology Department at Shiraz University. Grant number: 1403727.

Author contributions

Narges Kariminejad, Atiyeh Amindin, Adel Sepehr, and Hamid Reza Pourghasemi designed the experiments, analyzed the results, ran models, wrote, and reviewed the entire manuscript.

Funding

This project has been funded by the Office of Science and Technology Interactions, Research and Technology Department at Shiraz University (ShirazU Sci. Tech. Office). Grant number: 14032/10/9671.

Declarations

Competing interests

The authors declare no competing interests.

Additional information

Correspondence and requests for materials should be addressed to H.R.P.

Reprints and permissions information is available at www.nature.com/reprints.

Publisher's note Springer Nature remains neutral with regard to jurisdictional claims in published maps and institutional affiliations.